Dynamics of ATP-induced Calcium Signaling in Single Mouse Thymocytes

Paul E. Ross, George R. Ehring, and Michael D. Cahalan

Department of Physiology and Biophysics, University of California at Irvine, Irvine, California 92697

Abstract. Extracellular ATP (ATP_o) elicits a robust change in the concentration of intracellular Ca^{2+} ($[Ca^{2+}]_i$) in fura-2–loaded mouse thymocytes. Most thymocytes (60%) exposed to ATP_o exhibited a biphasic rise in $[Ca^{2+}]_i$; $[Ca^{2+}]_i$ rose slowly at first to a mean value of 260 nM after 163 s and then increased rapidly to a peak level of 735 nM. In many cells, a declining plateau, which lasted for more than 10 min, followed the crest in $[Ca^{2+}]_i$. Experiments performed in the absence of extracellular $[Ca^{2+}]_o$ abolished the rise in thymocyte $[Ca^{2+}]_i$, indicating that Ca^{2+} influx, rather than the release of stored Ca^{2+}, is stimulated by ATP_o. ATP_o-mediated Ca^{2+} influx was potentiated as the $[Mg^{2+}]_o$ was reduced, confirming that ATP^{4-} is the active agonist form. In the absence of $Mg^{2+}{}_o$, 3′-*O*-(4-benzoyl)benzoyl-ATP (BzATP) proved to be the most effective agonist of those tested. The rank order of potency for adenine nucleotides was $BzATP^{4-} > ATP^{4-} > MgATP^{2-} > ADP^{3-}$, suggesting purinoreceptors of the $P2X_7$/P2Z class mediate the ATP_o response. Phenotyping experiments illustrate that both immature ($CD4^-CD8^-$, $CD4^+CD8^+$) and mature ($CD4^+CD8^-$, $CD4^-CD8^+$) thymocyte populations respond to ATP. Further separation of the double-positive population by size revealed that the ATP_o-mediated $[Ca^{2+}]_i$ response was much more pronounced in large (actively dividing) than in small (terminally differentiated) $CD4^+CD8^+$ thymocytes. We conclude that thymocytes vary in sensitivity to ATP_o depending upon the degree of maturation and suggest that ATP_o may be involved in processes that control cellular differentiation within the thymus.

EXTRACELLULAR ATP (ATP_o)[1] and its metabolic products evoke physiological responses in virtually all tissues and cell types from central nervous to peripheral organ systems (for review see Dubyak and El-Moatassim, 1993; Harden et al., 1995). Tissues and isolated cells vary in sensitivity to purine agonists. Nucleotides (ATP, ADP, and AMP) and adenosine, the nucleoside product of ATP catabolism, elicit distinct responses in target cells by triggering P2 and P1 purinergic receptors, respectively (Burnstock, 1978). P2 purinoceptors can be further separated into two broad categories. The first group, divided into P2Y and P2U subtypes, couples nucleotide binding to effector molecules via G proteins. The second P2 category is comprised of nucleotide-sensitive ion channels and pores. ATP-gated P2 purinoceptors, designated $P2X_1$ through $P2X_6$ (cation channels) and $P2X_7$ (a dual function cation channel/pore), display extensive sequence identity (North, 1996) but disparate tissue distribution, biophysical properties, agonist profiles, and pharmacology ($P2X_1$, Valera et al., 1994; $P2X_2$-$P2X_6$, Collo et al., 1996; $P2X_7$, Surprenant et al., 1996). Moreover, P2X receptors functionally resemble acetylcholine- and serotonin-gated channels with respect to gating and ionic permeability but are structurally unique. Thus, nucleotides, together with acetylcholine, glutamate, GABA, glycine, and serotonin, are included in a small group of compounds that function as agonists for a structurally diverse set of ligand-gated ion channels and pores, as well as G protein-coupled receptors.

ATP_o elicits a broad spectrum of physiological changes in cells of the immune system. In mast cells, ATP release has been shown to mediate cell-to-cell signaling (Osipchuk and Cahalan, 1992). In lymphocytes, ATP_o triggers cellular depolarization, greater permeability to small organic molecules (<400 D; Wiley et al., 1993; Chused et al., 1996), and a rise in the concentration of intracellular Ca^{2+} ($[Ca^{2+}]_i$; El-Moatassim et al., 1987; Wiley and Dubyak, 1989). The ATP_o-mediated rise in $[Ca^{2+}]_i$ modifies the functional properties of thymocytes via DNA synthesis (Gregory and Kern, 1978, 1981; Ikehara et al., 1981) and blastogenesis (El-Moatassim et al., 1987). Moreover, an increase in $[Ca^{2+}]_i$ has been linked to programmed cell death in thymocyte populations; Ca^{2+} release from intracellular stores evoked by thapsigargin, a microsomal Ca^{2+}-ATPase inhib-

Please address all correspondence to Dr. Cahalan, Department of Physiology and Biophysics, University of California at Irvine, Irvine, CA 92697. Tel: (714) 824-7776; Fax: (714) 824-8540; E-mail: mcahalan@uci.edu

1. *Abbreviations used in this paper*: ATP_o, extracellular ATP; BzATP, benzoyl-ATP; $[Ca^{2+}]_i$, intracellular calcium concentration; $[Ca^{2+}]_o$, extracellular calcium concentration; MHC, major histocompatibility proteins; TCR, T-cell receptor.

itor, triggers the DNA fragmentation correlated with thymocyte apoptosis (Jiang et al., 1994; Zhivotovsky et al., 1994).

Based upon a sensitivity profile for purine agonists and pharmacological agents, lymphocytes are not believed to possess G protein-linked purinoceptors (El-Moatassim et al., 1989*b*). Rather, lymphocytes and related cell lines express purinoceptors of the ion channel/pore subtype ($P2X_7$). This ATP-gated pathway, originally termed P2Z (Gordon, 1986), has been characterized in mast cells (Cockcroft and Gomperts, 1979*a*; Tatham and Lindau, 1990), transformed 3T3 fibroblasts (Heppel et al., 1985), macrophages (Buisman et al., 1988), parotid acinar cells (Soltoff et al., 1992), and phagocytic cells of the thymic reticulum (Coutinho-Silva et al., 1996). During whole cell patch–clamp experiments, putative P2Z channels in human B lymphocytes (Bretschneider et al., 1995) and rat peritoneal macrophages (Naumov et al., 1995) exhibit rapid activation kinetics when exposed to ATP_o. The ATP_o response depends critically upon extracellular divalent cations (Mg^{2+} and Ca^{2+}), such that cellular depolarization and membrane permeability are greatest in divalent-free media. The ability of Mg^{2+}- and Ca^{2+}–ATP complexes to reduce receptor occupancy by lowering the concentration of ATP^{4-}, the effective form of the nucleotide agonist, is a hallmark of $P2X_7$/P2Z purinoceptor physiology (Cockcroft and Gomperts, 1979*b*).

In this study, we examined the dynamics of $[Ca^{2+}]_i$ changes elicited by ATP_o at the single-cell level in fura-2–loaded thymocytes. To our surprise, we found that the ATP_o-mediated $[Ca^{2+}]_i$ increase varies significantly between individual cells. Moreover, the kinetics of the rise in $[Ca^{2+}]_i$ at the single-cell level is characterized by a biphasic time course that is not detectable in average profiles. To correlate stages of thymocyte development with the degree of sensitivity to ATP_o, we measured the surface expression of specific T-lymphocyte markers, CD4 and CD8, before performing Ca^{2+}-imaging experiments. Our data illustrate that thymocytes vary in sensitivity to ATP_o depending upon level of maturation and degree of blastogenesis. Small, terminally differentiated, $CD4^+CD8^+$ thymocytes were least sensitive to ATP_o, while 90% of the single-positive ($CD4^+CD8^-$ or $CD4^-CD8^+$) cells, believed to be the immediate precursors of mature peripheral T-lymphocytes, exhibited a robust, ATP_o-dependent rise in $[Ca^{2+}]_i$. The in vitro data we have gathered suggest that ATP_o may drive thymocyte differentiation in the intact thymus.

Materials and Methods

Preparation of Cells and Fura-2 Loading

Intact thymus glands were extracted from 4–8-wk-old female BALB/c mice (The Jackson Laboratory, Bar Harbor, Maine). After gentle dissociation of the thymus between two frosted microscope slides, thymocytes were washed free in RPMI-1640 media (GIBCO BRL, Gaithersburg, MD) supplemented with 10% fetal calf serum (JR Scientific, Woodland, CA), 25 mM Hepes, and 2 mM glutamine. Thymocytes in suspension were centrifuged at 350 *g* for 10 min, resuspended in complete RPMI to 5×10^6 cells/ml, and then stored for <15 min before dye loading. Cells were maintained at 22°C during preparation, storage, dye loading, phenotyping, and experiments.

Thymocytes were loaded with 3 μM fura-2/AM (Molecular Probes, Inc., Eugene, OR) for 20 min. The cells were then washed three times with RPMI/10% FCS and stored in the dark. The loss of dye and the sequestration of fura-2 into intracellular compartments was minimal during storage (typically <6 h), as revealed by subsequent experiments. Thymocyte isolation and Ca^{2+}-imaging experiments were always performed on the same day.

Chemicals and Solutions

Thymocytes were bathed in mammalian Ringer containing (in mM) 160 NaCl, 4.5 KCl, 2 $CaCl_2$, 1 $MgCl_2$, 5 Hepes, and 10 glucose, titrated to pH 7.4 with NaOH (310 mOsmol kg^{-1}). $MgCl_2$ and $CaCl_2$ were omitted from divalent free solutions; Mg- and Ca-free solutions were unbuffered with respect to divalents. Immediately before experiments, nucleotides were added to bathing solutions. Solution pH was readjusted to 7.4 after nucleotide addition. All chemicals, including the nucleotides 3′-*O*-(4-benzoyl) benzoyl-ATP (BzATP), Na_2ATP, MgATP, and NaADP, were obtained from Sigma Chemical Co. (St. Louis, MO).

Fura-2 Imaging and Calibration

Fura-2 loaded thymocytes were allowed to settle on poly-D-lysine-(1 mg/ml) coated #0 coverslips (#0 red Label; Thomas Scientific, Swedesboro, NJ) for 10 min and then washed with Ringer on the stage of a fluorescent microscope (Axiovert 35; Zeiss, Inc., Oberkochen, Germany). Illumination was provided by a xenon arc-lamp (Zeiss, Inc.) and transmitted through a filter wheel unit (λ10; Axon Instruments, Inc., Foster City, CA) containing 360- and 380-nm excitation filters. The filtered light was reflected by a 400-nm dichroic mirror through a 100× oil-immersion objective to illuminate cells. Emitted light >480 nm was received by a SIT camera (C2400; Hamamatsu Photonics, Bridgewater, NJ) and the video information relayed to an image processing system (Videoprobe; ETM Systems, Irvine, CA). Full field-of-view 8-bit images, averaged over 16 frames, were collected at 360- and 380-nm wavelengths. Digitally stored 360/380 ratios were constructed from background-corrected 360- and 380-nm images. Single-cell measurements of $[Ca^{2+}]_i$ were calculated from the 360/380 ratios using the equation of Grynkiewicz et al. (1985) and a K_d of 250 nM for fura-2. The minimum fluorescence value at 380 nm and the minimum 360/380 ratio were measured in single cells after incubation for 10 min in Ca^{2+}-free Ringer containing 2 mM EGTA. Lymphocytes were then superfused with Ringer containing 1 μM thapsigargin (LC Services, Woburn, MA), 5 μM ionomycin (Sigma Chemical Co.), and 10 mM Ca^{2+} to evaluate the maximum fluorescence at 380 nM and the maximum 360/380 ratio.

Lymphocyte Phenotyping

The presence or absence of CD4 and CD8 molecules provides a measure of T-lymphocyte maturation within the thymus (Scollay et al., 1988). An early stage of thymocyte development is indicated by the absence of both CD4 and CD8 surface markers. These cells, designated $CD4^-CD8^-$ (double negatives), differentiate into $CD4^+CD8^+$ thymocytes (double positives). During the double-positive stage, thymocytes are positively selected for proper recognition between T cell receptor (TCR) and self major histocompatibility proteins (MHC). Anomalously high affinity interactions between TCR and MHC target cells for negative selection. The majority of thymocytes (95%) are not positively selected and die by neglect within the cortex of the thymus by a process termed apoptosis (Osborne, 1996). Apoptotic thymocytes are small and terminally differentiated. Thymocytes receiving the proper signals continue to develop into medium and large size double positives, eventually giving rise to single-positive T cell populations. Therefore, five classes of thymocytes can be identified based upon cell size and the expression of CD4 and CD8: double negatives, small and large double positives, and single positives.

We identified thymocyte surface phenotype before performing Ca^{2+} imaging for several experiments. Thymocytes were labeled with CD4 (L3T4) and CD8 (Lyt-2) monoclonal antibodies (Pharmingen, San Diego, CA) conjugated with phycoerythrin (PE) or FITC, respectively. 30-μl aliquots of thymocytes (1.5×10^5 cells) were incubated at 22°C with 5 μg/ml anti–CD4-PE, 5 μg/ml anti–CD8-FITC, and 3 μM fura-2/AM for 20 min. After staining, cells were washed three times in complete RPMI and resuspended to a final volume of 400 μl; 50 μl aliquots of stained cells were adhered to poly-D-lysine–coated coverslip chambers for 10 min before experiments.

A xenon light source was used to evaluate the CD4/CD8 phenotype of labeled thymocytes. The filter sets used for phenotyping were optimized for the separation of PE and FITC signal, while excluding fura-2 fluorescence. The PE set contained a 510- to 560-nm excitation filter, a 580-nm

dichroic beam splitter, and a 590-nm-long pass emission filter. The FITC set included a 450- to 490-nm excitation filter, a 510-nm dichroic beam splitter, and a 40-nm-wide, 540-nm emission filter. Red (CD4/PE) and green (CD8/FITC) fluorescence images of labeled cells were collected before $[Ca^{2+}]_i$ measurements with a black and white SIT camera. The use of narrow filters for fura-2 excitation prohibited PE and FITC fluorescence contamination during $[Ca^{2+}]_i$ measurements. Cells were classified by visual inspection into four phenotypic categories by toggling between fluorescence images after experiments: (*a*) lymphocytes exhibiting fluorescence using both filter sets (double positives); (*b*) cells exhibiting only PE fluorescence ($CD4^+CD8^-$ single positives); (*c*) thymocytes exhibiting only FITC fluorescence ($CD4^-CD8^+$ single positives); and (*d*) unlabeled thymocytes showing no fluorescence (double negatives) that only appeared in fura-2 $[Ca^{2+}]_i$ images. Alternatively, PE and FITC were color coded and overlaid to produce a single composite image (see Fig. 4 *A*). The volume (V) of each thymocyte was determined from surface area (S) outlines using NIH Image v1.60 (a Macintosh computer program written by Wayne Rasband at the National Institutes of Health and available from the Internet by anonymous ftp from zippy.nimh.nih.gov or on floppy disc from NTIS, 5285 Port Royal Rd., Springfield, VA 22161; part no. PB93-504868) and the equation $V = (S)^{3/2}$. For this relationship to be valid, thymocytes must remain spherical during experiments. Cell outlines in PE and FITC images were used to determine the size of single- and double-positive thymocytes, while the volume of double negatives was determined from fura-2 $[Ca^{2+}]_i$ images. Double-positive cells were further subdivided into large (actively dividing) and small (terminally differentiated) diameter classes.

Data Analysis

Numerical values for single-cell $[Ca^{2+}]_i$ traces were analyzed with Igor Pro, an Apple Macintosh computer program (v3.02; WaveMetrics, Inc., Lake Oswego, OR). Statistical analysis was performed on data sets using Excel v5.0 (Microsoft, Redmond, WA), SuperAnova v1.11 (Abacus Concepts, Inc., Berkeley, CA), and Systat v5.1 (Systat Inc., Evanston, IL). The composite pseudocolor overlay presented in Fig. 4 *A* was generated with Photoshop v4.0 (AdobeSystems Inc., San Jose, CA). Data are reported as mean ±SD. Analysis of variance (ANOVA) was used to compare mean values. Pairs of means were considered statistically different if P was <0.05.

Results

ATP_o Induces a Rise in $[Ca^{2+}]_i$ in Mouse Thymocytes

ATP_o is recognized as an effective modulator of $[Ca^{2+}]_i$ levels within lymphocytes (El-Moatassim et al., 1987; Pizzo et al., 1991; Wiley et al., 1993; Chused et al., 1996). In addition to activating Ca^{2+} influx pathways, ATP_o is thought to trigger the opening of pores in the plasma membrane of thymocytes, which allow molecules of at least 200 D to permeate (Pizzo et al., 1991; Nagy et al., 1995; Chused et al., 1996). In our experiments, thymocyte ATP_o-gated pores are narrow enough to restrict the passage of fura-2^{4-} (832 D), since we did not observe a decrease in fluorescence intensity at 360 nM during measurements (data not shown). Fig. 1 shows that the majority of thymocytes (58%) exposed to 1 mM Na_2ATP exhibit a robust change in $[Ca^{2+}]_i$ at the single-cell level. In Fig. 1 *A*, $[Ca^{2+}]_i$ profiles for all thymocytes in a typical experiment illustrate the variability of the ATP_o response. From a resting $[Ca^{2+}]_i$ level of 131 ± 13 nM (n = 25 experiments, 2814 cells), ATP_o triggered a rise in $[Ca^{2+}]_i$ to peak levels averaging 735 ± 230 nM (n = 3 experiments, 217 cells). A slowly declining plateau persisted in many cells for more than 10 min after peak $[Ca^{2+}]_i$ (Fig. 1 *B*). Because the time of initiation and amplitude of the rise in thymocyte $[Ca^{2+}]_i$ was variable, the average time course over the length of the experiment is broadened (Fig. 1 *C*). Average $[Ca^{2+}]_i$ measurements by spectrofluorimetry (El-Moatassim et al., 1987; Pizzo et al., 1991) and flow cytometry (Nagy et al., 1995; Chused et al., 1996) of ATP_o-treated thymocytes are identical in profile with the upper graph in Fig. 1 *C*.

A narrow band centered at 260 ± 29 nM marks the position of a distinct inflection in the $[Ca^{2+}]_i$ curves of ATP_o-sensitive thymocytes (Fig. 2 *A*). The inflection gave these graphs a well defined biphasic character and signaled a faster rate of rise in $[Ca^{2+}]_i$ averaging 19 ± 19 nM/s. As illustrated by three single-cell traces in Fig. 2 *A*, neither the length of time before reaching the threshold, nor the peak value after the inflection, correlated with the level of $[Ca^{2+}]_i$ at which the transition occurred. These observations are presented graphically in Fig. 2 *B*; while peak thymocyte $[Ca^{2+}]_i$ levels are scattered randomly, inflection point $[Ca^{2+}]_i$ levels are tightly clustered.

The $[Ca^{2+}]_i$ Rise Is Stimulated Most Potently by $BzATP_o$

To identify the type of purinoceptor expressed in thymocytes, we tested the efficacy of various nucleotides and ATP analogs in raising $[Ca^{2+}]_i$. Thymocytes were least sensitive to ADP_o; only 20% (n = 4 experiments, 303 cells) of the cells exhibited a rise in $[Ca^{2+}]_i$ after the application of 1 mM NaADP (data not shown). $[Ca^{2+}]_i$ time courses were similar for ADP_o- and ATP_o-sensitive thymocytes, suggesting that both nucleotides stimulate a single purinoceptor subtype. BzATP, in the absence of extracellular Mg^{2+}, proved to be the most effective agonist and elicited a rapid rise in thymocyte $[Ca^{2+}]_i$ when used at 100 μM (Fig. 3 *A*). Single-cell $[Ca^{2+}]_i$ profiles evoked by $BzATP_o$, ATP_o (compare Fig. 3 *B* with 2 *A*), and ADP_o were comparable; these agonists caused a biphasic $[Ca^{2+}]_i$ rise in thymocytes after crossing a distinct threshold (Fig. 3 *C*). On average, 65 ± 2% (n = 2 experiments, 147 cells) of the $BzATP_o$-treated cells exhibited a slow rise in $[Ca^{2+}]_i$ to a threshold level of 263 ± 33 nM. Above the inflection point, $[Ca^{2+}]_i$ increased at a rate of 17 ± 17 nM/s and reached a peak averaging 702 ± 249 nM. Similarly, in transformed fibroblasts (Gonzalez et al., 1989), parotid acinar cells (Soltoff et al., 1992), macrophages (El-Moatassim and Dubyak, 1992; Nuttle et al., 1993), and B-lymphocytes (Wiley et al., 1994), $BzATP_o$ proved to be the most effective purinergic agonist. Since BzATP is believed to be specific for $P2X_7$/P2Z purinoceptors and all three nucleotides used in our experiments produced an equivalent $[Ca^{2+}]_i$ time course, we conclude that purinoceptors of the ion channel/pore subtype are expressed in thymocytes.

Phenotypic Classes of Thymocytes Differ in Sensitivity to ATP_o

We examined the surface expression of CD4 and CD8 molecules with fluorescently labeled antibodies to address the hypothesis that stages of thymocyte maturation correlate with sensitivity to ATP_o. In Fig. 4 *A*, fluorescence images of anti–CD4-PE and anti–CD8-FITC labeled thymocytes were color coded and overlayed to aid phenotyping. The fluorescence intensity of individual cells varied, indicating unequal surface expression of CD4 and CD8. Most cells in

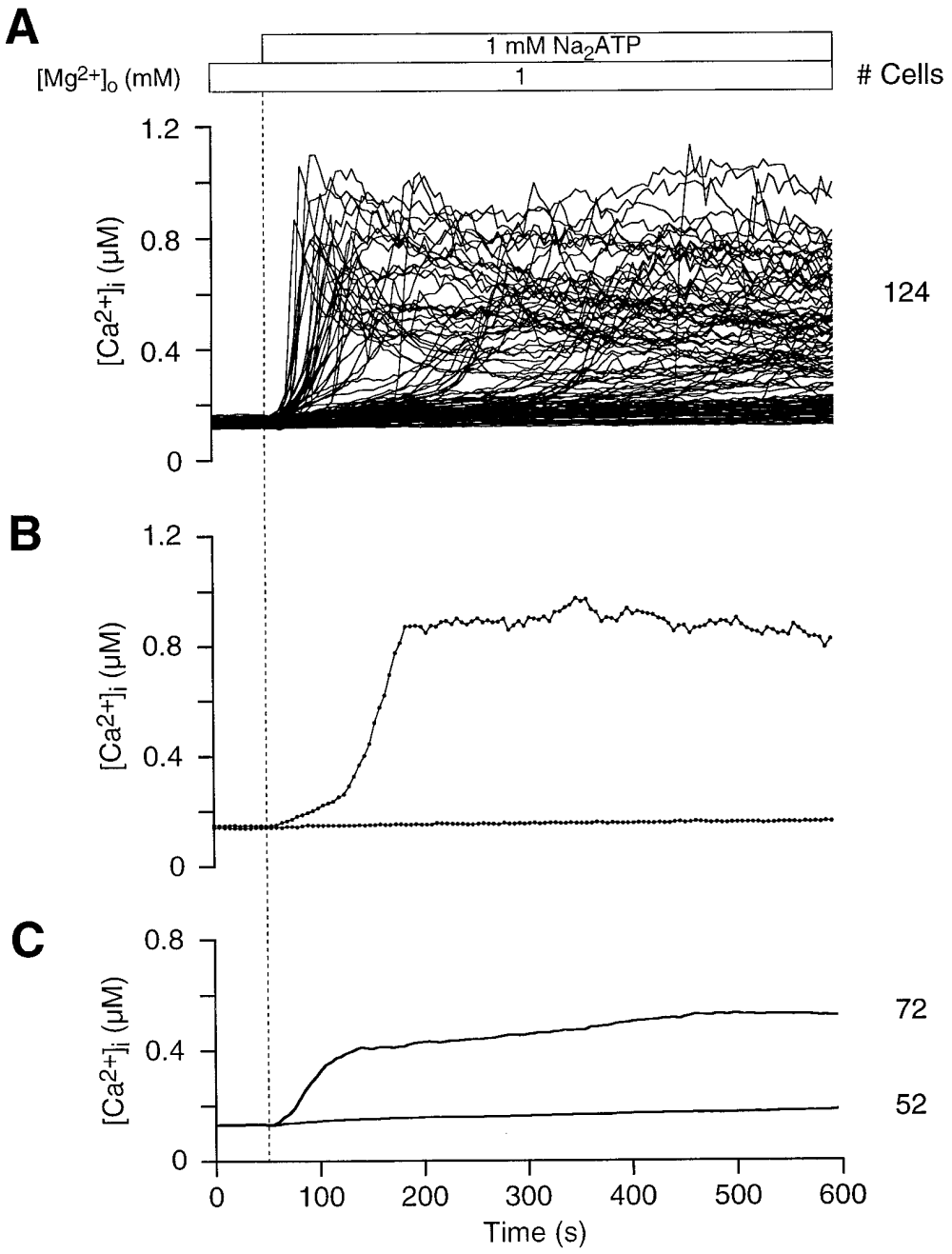

Figure 1. Mouse thymocytes exhibit an ATP_o-induced rise in $[Ca^{2+}]_i$. (*A*) $[Ca^{2+}]_i$ is plotted against time for all cells in a typical experiment to illustrate the range of responses to ATP_o at the single-cell level. Superfusion of ATP_o began at 50 s, as indicated by the application bar above the graph and the vertical dotted line. During the application of ATP_o, the bath solution was exchanged over a period of 20 s. The time to peak $[Ca^{2+}]_i$ and the level of $[Ca^{2+}]_i$ at the crest varied significantly between thymocytes. This experiment was performed with normal Ringer's solution containing 1 mM $Mg^{2+}{}_o$. (*B*) Two populations of thymocytes can be identified by sensitivity to ATP_o; 58% of the cells show a rise in $[Ca^{2+}]_i$, while the balance exhibits little change in $[Ca^{2+}]_i$ over the length of the experiment. Two representative $[Ca^{2+}]_i$ profiles illustrate ATP_o-sensitive and -insensitive thymocytes at the single-cell level. The time courses include experimental data (*black dots*) recorded at 5-s intervals (experiment 71295-2; Cells 119 and 126). (*C*) Average $[Ca^{2+}]_i$ is plotted against time for thymocytes exhibiting an ATP_o-induced rise in $[Ca^{2+}]_i$ and for nonresponsive cells.

PE and FITC composite images correspond to small, double-positive thymocytes; these terminally differentiated thymocytes constitute 50% of the cells in a typical thymus preparation (Table I). Larger double-positive thymocytes, representing 13% of the total population, were easily discriminated from smaller cells based upon surface area outlines in PE and FITC images. After recording fluorescence images, thymocytes were treated with 100 μM $BzATP_o$. A snapshot pseudocolor image of $[Ca^{2+}]_i$ within cells, acquired 100 s after $BzATP_o$ application, is displayed in Fig. 4 *B*. Selected single-cell $[Ca^{2+}]_i$ profiles, representing the five thymocyte populations, are illustrated in Fig. 4 *C*. As a group, the small, terminally differentiated, double-positive thymocytes were least responsive to $BzATP_o$, while $CD4^-CD8^+$ cells exhibited the most robust $[Ca^{2+}]_i$ rise. Furthermore, the onset of the $BzATP_o$ response correlates with phenotype; $[Ca^{2+}]_i$ in $CD4^-CD8^+$ thymocytes reach inflection and peak levels almost twice as fast as small $CD4^+CD8^+$ cells. Fig. 5, *A* and *B* display Gaussian curves fitted to volume histograms for the five thymocyte populations. Small double-positive thymocytes fell within a narrow volume distribution, while larger double-positive cells were scattered over a wider range of sizes (Fig. 5 *A*). Similarly, single-cell volumes of double-negative and single-positive classes were dispersed (Fig. 5 *B*). Table I and Fig. 5 *C* summarize average $[Ca^{2+}]_i$ data for the five thymocyte

Table I. Maturational Stages in Thymocyte Development Show Distinct $[Ca^{2+}]_i$ Response Profiles

CD4/CD8	+/+ (Small)	+/+ (Large)	−/−	+/−	−/+
Percentage of total	50	13	10	21	6
Percentage responding to ATP_o	44	67	67	93	85
Time of inflection (s)	302 ± 131	216 ± 89*	205 ± 87*	199 ± 92*	162 ± 69*
Inflection $[Ca^{2+}]_i$ level (nM)	296 ± 24	311 ± 40*	301 ± 59	278 ± 43*	318 ± 45*
Rate of rise after inflection (nM/s)	10 ± 8	12 ± 8	25 ± 22*	43 ± 29*	37 ± 27*
Time of peak $[Ca^{2+}]_i$ (s)	397 ± 143	315 ± 127*	304 ± 135*	238 ± 114*	208 ± 93*
Peak $[Ca^{2+}]_i$ level (nM)	614 ± 166	735 ± 195*	941 ± 180*	892 ± 218*	913 ± 195*
Volume (fl)	178 ± 28	328 ± 72*	394 ± 194*	251 ± 89*	275 ± 99*

Mean values were compared with a one-way analysis of variance and the statistical difference between pairs of means evaluated with a Tukey-Kramer post-hoc test. Data collected from 10 experiments: +/+ (small) phenotype, 269 cells; +/+ (large) phenotype, 70 cells; 2/2 phenotype, 52 cells; +/− phenotype, 1134 cells; −/+ phenotype, 34 cells (experiments 9796-2 though -6, 9896-1 through -4, and 9896-10). *Values significantly different ($P < 0.05$) from $CD4^+$ $CD8^+$ phenotype.

populations. These data indicate that actively dividing thymocytes are most sensitive to extracellular nucleotides, while cells destined for apoptosis are least responsive.

The ATP_o-mediated Rise in $[Ca^{2+}]_i$ Does Not Occur in the Absence of $Ca^{2+}{}_o$

The nucleotide-dependent rise in thymocyte $[Ca^{2+}]_i$ may be generated by Ca^{2+} influx across the plasma membrane or Ca^{2+} release from intracellular reservoirs. We examined the mechanism leading to the $[Ca^{2+}]_i$ response by performing experiments under $Ca^{2+}{}_o$-free conditions. In Fig. 6, thymocytes were treated with 100 μM $BzATP_o$ in Ca-free media for 100 s. A slight rise in $[Ca^{2+}]_i$ was registered in a few thymocytes in zero $Ca^{2+}{}_o$ (Fig. 6 *A*), however the majority of cells remained at or near pre-agonist $[Ca^{2+}]_i$

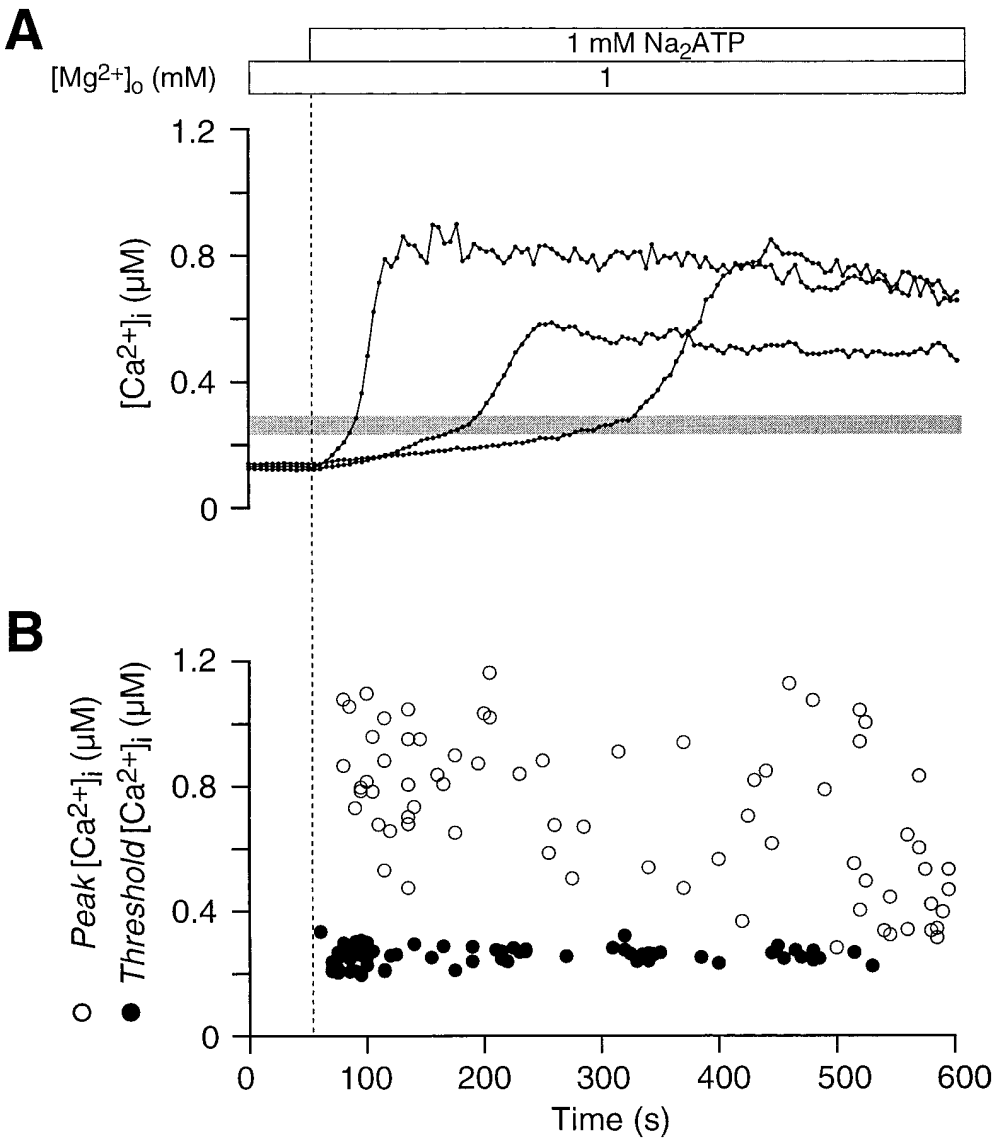

Figure 2. ATP_o induces a biphasic $[Ca^{2+}]_i$ rise in thymocytes. (*A*) In most ATP_o-sensitive thymocytes, $[Ca^{2+}]_i$ rises slowly at first, reaches a threshold, and then increases rapidly; three representative single-cell traces are displayed. The threshold $[Ca^{2+}]_i$ level, signified by an inflection point in these curves, occurs over a narrow range. The gray bar across the graph is centered over the mean, while the vertical thickness of the bar indicates ±SD (experiment 71295-2; Cells 27, 41, and 61). (*B*) Peak $[Ca^{2+}]_i$ and the $[Ca^{2+}]_i$ level at the inflection point are plotted against time for 72 cells. The narrow band of data points denoting threshold $[Ca^{2+}]_i$ contrasts sharply with the scattered distribution of peak $[Ca^{2+}]_i$ values.

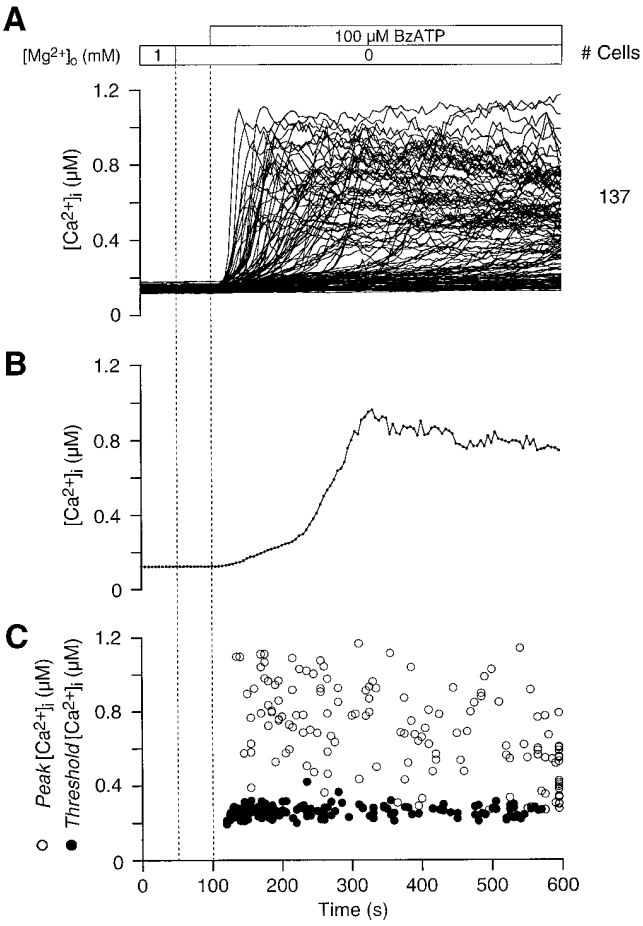

Figure 3. $BzATP_o$ potently stimulates Ca^{2+} influx in thymocytes. (*A*) Of the nucleotides tested, $BzATP_o$ proved to be the most effective nucleotide agonist stimulating a rise in thymocyte $[Ca^{2+}]_i$. Individual thymocytes exhibit a nonuniform $[Ca^{2+}]_i$ response to 100 μM $BzATP_o$; 137 single-cell traces are displayed. (*B*) The single-cell $[Ca^{2+}]_i$ rise evoked by $BzATP_o$ closely resembles the ATP_o-elicited response. A representative single-cell trace during $BzATP_o$ application is shown. (Experiment 71595-7; Cell 30.) (*C*) The level of $[Ca^{2+}]_i$ at the peak and at the inflection point for 147 $BzATP_o$-sensitive thymocytes are plotted against time. Peak $[Ca^{2+}]_i$ levels show wide dispersion while threshold values are tightly clustered (experiments 71595-7 and 71595-23).

levels. $Ca^{2+}{}_o$ readdition to $BzATP_o$-treated thymocytes caused a vigorous rise in $[Ca^{2+}]_i$, indicating that Ca^{2+} influx dominates the response. We have shown previously that stored Ca^{2+} levels remain high in thymocytes bathed in Ca-free media over comparable incubation periods (Ross and Cahalan, 1995). This observation excludes the possibility that in zero $Ca^{2+}{}_o$, intracellular Ca^{2+} stores may slowly empty below a level necessary to be registered upon subsequent release. Single-cell traces exhibit a biphasic time course followed by a declining plateau; an example is shown in Fig. 6 *B*. Grouped data illustrate that the brief period of $Ca^{2+}{}_o$ withdrawal does not significantly affect the subsequent $[Ca^{2+}]_i$ rise. Nevertheless, average $[Ca^{2+}]_i$ reaches the plateau level more slowly, which suggests that during the $Ca^{2+}{}_o$-free episode, purinergic receptors may become desensitized to nucleotides (Fig. 6 *C*). These data are consistent with previous studies showing that the activation of $P2X_7$/P2Z purinoceptors stimulates Ca^{2+} influx and not Ca^{2+} release in thymocytes (El-Moatassim et al., 1989*b*; Pizzo et al., 1991; Chused et al., 1996).

Ca^{2+} Influx and the Potency of ATP_o Increase as $Mg^{2+}{}_o$ Is Reduced

Extracellular Mg^{2+} and Ca^{2+} ions are thought to play an important role in regulating ATP-mediated responses in mast cells (Cockcroft and Gomperts, 1979*b*) and T lymphocytes (Steinberg and Di Virgilio, 1991). We examined the ability of Mg^{2+} to affect ATP_o-mediated $[Ca^{2+}]_i$ responses in thymocytes by reducing $[Mg^{2+}]_o$ from 2 to 1 mM (Fig. 7). Approximately 19% of the cells showed a rise in $[Ca^{2+}]_i$ in 2 mM $[Mg^{2+}]_o$; an additional 41% exhibited a rise in $[Ca^{2+}]_i$ as $[Mg^{2+}]_o$ was lowered to 1 mM. All of the thymocytes in the original 19% exhibited a further rise in $[Ca^{2+}]_i$ when $[Mg^{2+}]_o$ was decreased. These results agree with the hypothesis that ATP^{4-} is the active agonist form for $P2X_7$/P2Z purinoceptors on thymocytes.

We also examined purinoceptor activity after agonist withdrawal (Fig. 8). A $[Ca^{2+}]_i$ rise was evoked by 1 mM MgATP in the presence of 1 mM $[Mg^{2+}]_o$. Agonist was then withdrawn, which caused $[Ca^{2+}]_i$ to decrease, as expected. Removing $Mg^{2+}{}_o$ resulted in an unanticipated rise in $[Ca^{2+}]_i$, in the absence of agonist, indicating that purinoceptors remain occupied by ATP. We believe this ATP to be initially in the form of $MgATP^{2-}$. The removal of $Mg^{2+}{}_o$ liberates the more potent ATP^{4-} by dissociation, which then is registered as rising $[Ca^{2+}]_i$ as more purinoceptors are activated. Subsequent addition of 100 μM $BzATP_o$ further stimulates purinoceptor activity.

Given these data, we conclude that $MgATP^{2-}$ can bind to purinoceptors. However, it is unclear whether $MgATP^{2-}$ directly activates the receptors or if low concentrations of ATP^{4-}, in equilibrium with inactive $MgATP^{2-}$, are actually responsible for purinoceptor operation. Assuming that $MgATP^{2-}$ has a direct effect, the rank order of potency for stimulation of Ca^{2+} influx in thymocytes by adenine nucleotides is $BzATP^{4-} > ATP^{4-} > MgATP^{2-} > ADP^{3-}$.

Discussion

We have characterized ATP_o-mediated $[Ca^{2+}]_i$ responses in thymocytes at the single-cell level. The $[Ca^{2+}]_i$ profile is distinguished by a biphasic time course with a distinct inflection (Figs. 1, 2, and 3). The rise in $[Ca^{2+}]_i$ is generated primarily by Ca^{2+} influx, with Ca^{2+} release from stores playing little if any role (Fig. 6). The response is potently stimulated by $BzATP_o$, supporting the conclusion that thymocytes express purinoceptors of the $P2X_7$/P2Z variety (Fig. 3). Interestingly, actively dividing thymocytes are preferentially targeted by extracellular nucleotides, such that single-positive cells exhibit the most pronounced $[Ca^{2+}]_i$ increase (Fig. 4 and Table I). More than half of the small, terminally differentiated, double-positive thymocytes were insensitive to the effects of ATP_o. Of the small double-positive cells that did respond, peak $[Ca^{2+}]_i$ levels were significantly less than those in all other classes of thymocytes (Table I). Consistent with other researchers, we find Mg^{2+}-free ATP^{4-} to be the active agonist form (Fig.

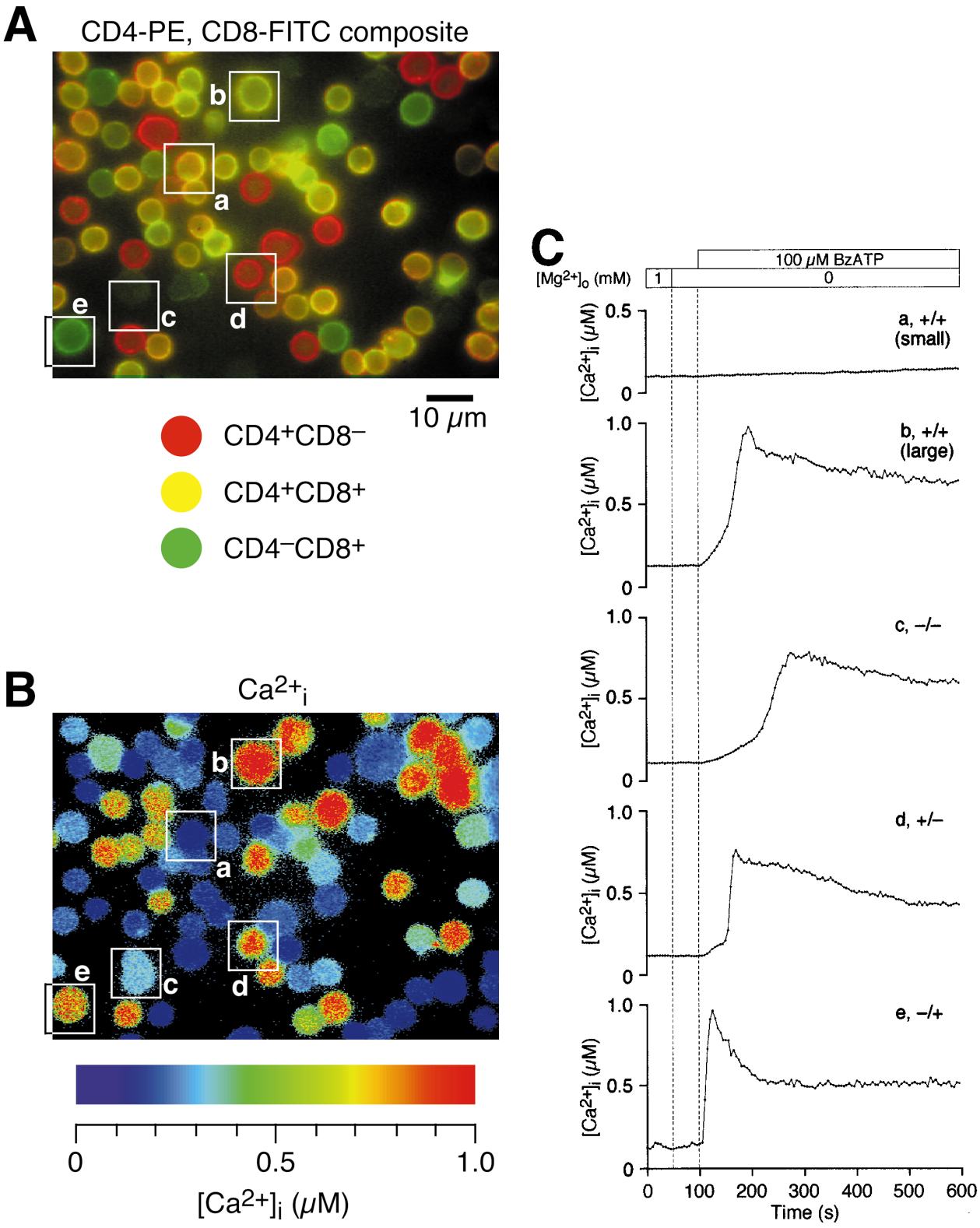

Figure 4. Sensitivity to $BzATP_o$ correlates with stages of thymocyte maturation. (*A*) Thymocytes were labeled with anti-CD4-PE (*red*) and anti-CD8-FITC (*green*) before $BzATP_o$ addition. Black and white fluorescence images were recorded, color coded, and then superimposed to aid phenotyping of labeled thymocytes. The surface expression of CD4 and CD8 are variable, leading to unequal fluorescence intensities emanating from $CD4^+CD8^-$ (*red*), $CD4^+CD8^+$ (*yellow*), and $CD4^-CD8^+$ (*green*) thymocytes. The bright spot near the center of the image is caused by an out of focus cell above the layer of thymocytes attached to the coverslip. (*B*) A pseudocolor display of $[Ca^{2+}]_i$ within fura-2–loaded thymocytes 100 s after $BzATP_o$ application. Below the panel is a rainbow bar correlating color with $[Ca^{2+}]_i$. $[Ca^{2+}]_i$ profiles of thymocytes within boxes are displayed in *C*. These identification boxes, which in some cases overlap with adjacent cells, were not used to evaluate thymocyte $[Ca^{2+}]_i$ levels. (*C*) Representative single-cell $[Ca^{2+}]_i$ profiles for five populations of thymocytes. Small, terminally differentiated, double-positive thymocytes are least responsive, while 90% of the $CD4^-CD8^+$ thymocytes treated with $BzATP_o$ exhibit a rapid rise in $[Ca^{2+}]_i$ (experiment 9896-2; +/+, Cell 31; +/+ [*large*], Cell 77; −/−, Cell 64; +/−, Cell 53; −/+, Cell 26).

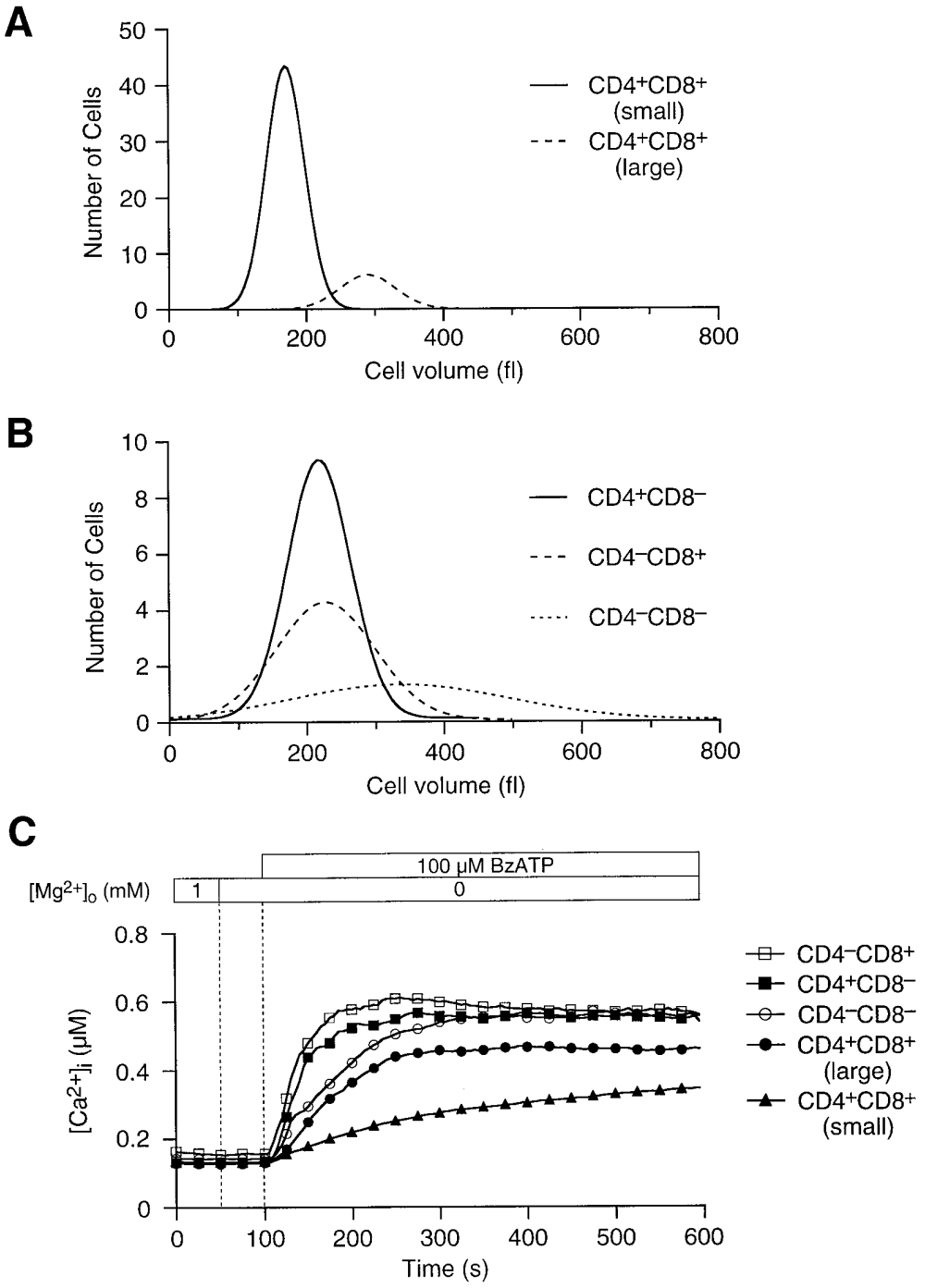

Figure 5. Volume distribution of phenotype subclasses, which show distinct $BzATP_o$-induced $[Ca^{2+}]_i$ response profiles. (*A*) Gaussian curves fitted to volume-frequency histograms illustrate the separation of double-positive thymocytes into two distinct populations. Single-cell volumes, in femtoliters (*fl*), were calculated from surface area outlines of cells appearing in anti–CD4-PE and anti–CD8-FITC images. (*B*) Size distribution for double-negative and single-positive thymocytes. Single-cell volumes for $CD4^-CD8^-$ cells were scattered over a wide range of values, while those for single positives were more tightly clustered. (*C*) Average $[Ca^{2+}]_i$ profiles for the five thymocyte populations. $CD4^-CD8^+$ thymocytes exhibited a strong $[Ca^{2+}]_i$ response, while small double-positive cells were least sensitive to 100 μM $BzATP_o$ (experiments 9796-2 through -6, 9896-1 through -4, and 9896-10).

7). However, our results suggest that the $MgATP^{2-}$ complex binds to the receptor, and may remain bound even after agonist is washed from the bathing solution (Fig. 8).

Extracellular ATP Stimulates a Biphasic Rise in Thymocyte $[Ca^{2+}]_i$

By examining purinergic responses in thymocytes at the single-cell level, our work has revealed that $[Ca^{2+}]_i$ dynamics follow a more complicated profile than anticipated, based upon previous studies displaying average traces (El-Moatassim et al., 1987; Pizzo et al., 1991; Nagy et al., 1995; Chused et al., 1996). Earlier work conducted on thymocyte populations gave no indication of a biphasic time course, instead showing a smoothly rising profile. In contrast, single-cell measurements of thymocyte $[Ca^{2+}]_i$ consistently exhibit a slowly rising phase that leads to a distinct inflection, followed by a more rapid increase (Figs. 1, 2, and 3). This biphasic profile may be generated by several mechanisms. First, the initial rise in thymocyte $[Ca^{2+}]_i$ may appear slower due to a partial masking of influx by Ca^{2+} sequestration into intracellular organelles, Ca^{2+} extrusion through Ca^{2+}ATPases, and buffering by intracellular compounds. Saturation of these processes at a particular $[Ca^{2+}]_i$ level (the inflection point) may lead to the faster rising phase. Second, early Ca^{2+} influx through open path-

ways may induce other ATP-gated purinoceptors to open, or may act upon already open channels to trigger greater influx through positive feedback. Third, the activation of Ca^{2+}-activated K^+ channels (K_{Ca}; Mahaut-Smith and Mason, 1991) during early Ca^{2+} influx may hyperpolarize thymocytes and increase the driving force for Ca^{2+} through ATP-gated channels to generate the fast-rising phase. Membrane potential hyperpolarization, believed to be associated with the activity of K_{Ca} channels, has been observed when thymocytes are exposed to low concentrations of ATP_o (0.5 mM in Mg^{2+}-free buffer; Matko et al., 1993). However, higher ATP_o concentrations (1 mM) stimulate substantial depolarization (Pizzo et al., 1991; Matko et al., 1993; Chused et al., 1996). Finally, recent reports document the presence of $P2Y_2$ mRNA (mouse; Koshiba et al., 1997) and $P2X_1$ mRNA (rat; Chvatchko et al., 1996; Koshiba et al., 1997) in dexamethasone-treated thymocytes. In addition, the superantigen staphylococcal enterotoxin B upregulates $P2X_1$ mRNA expression and protein in mouse thymocytes (Chvatchko et al., 1996). Our data support the theory that mouse thymocytes normally express $P2X_7$/P2Z purinoceptors, given maximal sensitivity to $BzATP_o$ (Fig. 3) and $Mg^{2+}{}_o$ dependence (see below and Figs. 7 and 8). If two or more types of purinoceptors are coexpressed, then the biphasic profile we see may reflect the sequential activation of the multiple classes of nucleotide-gated receptors.

The biphasic nature of the $[Ca^{2+}]_i$ rise and the time course variability among individual cells complicated our efforts to develop reliable $[ATP]_o$–$[Ca^{2+}]_i$ response curves (data not shown). The generation of precise nucleotide concentration-response curves is also made problematic by the presence of surface ectonucleotidases, which degrade extracellular nucleotides rapidly, on $CD4^+CD8^-$, $CD4^-CD8^+$, and $CD4^-CD8^-$, but not $CD4^+CD8^+$ thymocytes (Dornand et al., 1986; however, Barankiewicz et al. [1988] report no ectonucleotidase activity in pooled thymocyte mixtures). Nevertheless, our data at the single-cell level provide new information concerning the dynamics of thymocyte $[Ca^{2+}]_i$ changes induced by ATP_o.

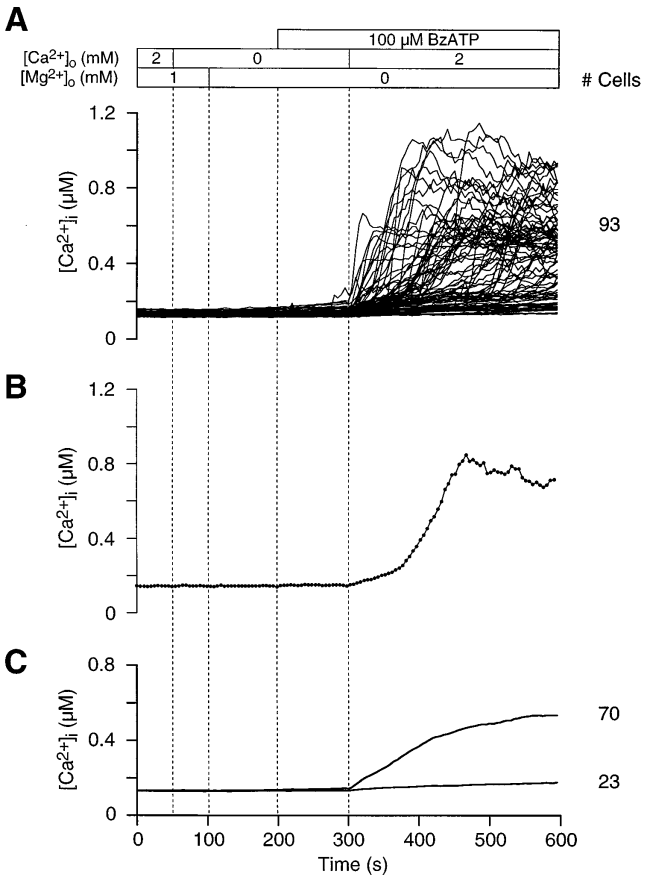

Figure 6. Ca^{2+} influx, rather than Ca^{2+} release from stores, is stimulated by $BzATP_o$. (*A*) A slight rise in $[Ca^{2+}]_i$ (<30 nM) was observed in a few $BzATP_o$-treated thymocytes bathed in Ca-free media, indicating that Ca^{2+} release from intracellular stores plays an insignificant role in the purinergic response. After $Ca^{2+}{}_o$ is reapplied, $[Ca^{2+}]_i$ rises quickly in 75% of the cells. Therefore, Ca^{2+} influx underlies the $BzATP_o$ response. (*B*) Thymocytes respond normally to $BzATP_o$ after $Ca^{2+}{}_o$ removal and readdition; a representative single-cell $[Ca^{2+}]_i$ time course is displayed (experiment 71595-21; Cell 78). (*C*) The average $[Ca^{2+}]_i$ course for $BzATP_o$-sensitive cells is slower to reach plateau levels, suggesting that purinergic receptors may become desensitized to $BzATP_o$ during the $Ca^{2+}{}_o$-free episode.

Ca^{2+} Influx through Thymocyte Purinoceptors Depends Critically on $Mg^{2+}{}_o$

One interpretation of the experiments presented in Figs. 7 and 8 is that ATP^{4-}, the active form of the agonist, is released from $MgATP^{2-}$ as $Mg^{2+}{}_o$ decreases. The increase in

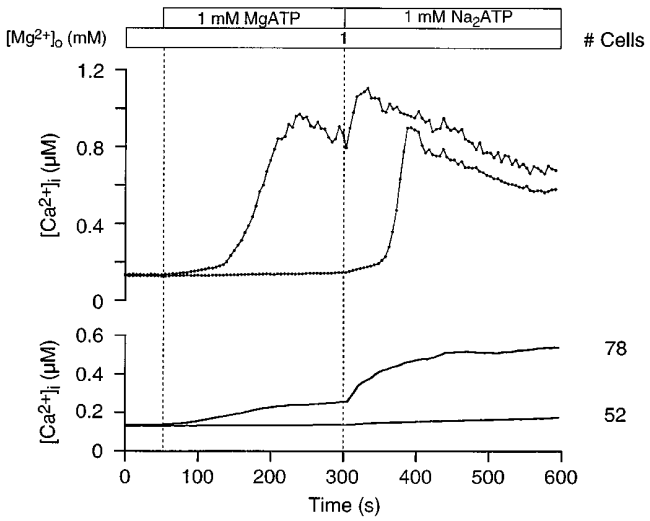

Figure 7. ATP_o-mediated Ca^{2+} influx in thymocytes is dependent upon $[Mg^{2+}]_o$. The number of thymocytes exhibiting an ATP_o-dependent rise in $[Ca^{2+}]_i$ increases as $[Mg^{2+}]_o$ is halved from 2 to 1 mM, suggesting that ATP^{4-}, rather than $MgATP^{2-}$, is the active form of the agonist. The top graph presents two representative single-cell traces that illustrate that the threshold of activation for the $[Ca^{2+}]_i$ rise varies between thymocytes. Interestingly, the reduction in $[Mg^{2+}]_o$ elicits a further rise in $[Ca^{2+}]_i$ in many cells. The lower graph displays average $[Ca^{2+}]_i$ in ATP_o-sensitive and -insensitive thymocytes. Three times as many thymocytes exhibit a rise in $[Ca^{2+}]_i$ as $[Mg^{2+}]_o$ is reduced. Reducing Mg^{2+} did not affect $[Ca^{2+}]_i$ levels within unresponsive thymocytes (experiment 71295-3; Cell 15 and 21).

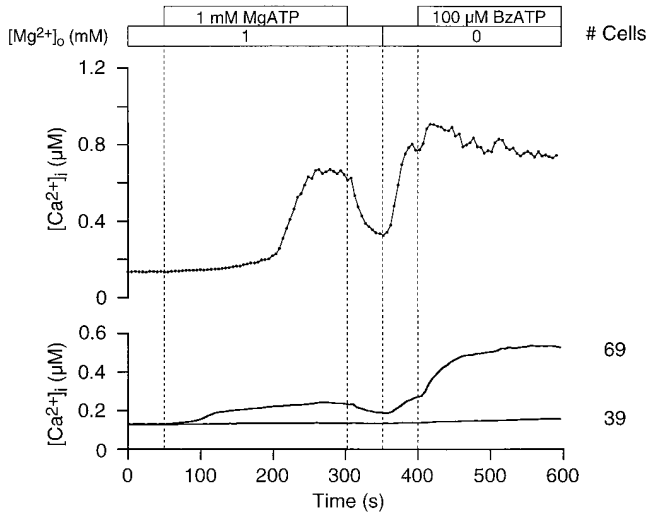

Figure 8. Thymocyte purinoceptors remain open after agonist withdrawal. Purinoceptors were activated by 1 mM MgATP in the presence of 1 mM $[Mg^{2+}]_o$. A rise in $[Ca^{2+}]_i$ was measured in 64% of the cells. Washing thymocytes with Ringer reduced $[Ca^{2+}]_i$ levels. Subsequent removal of all $Mg^{2+}{}_o$ caused $[Ca^{2+}]_i$ to rise, in spite of the absence of agonist. The addition of 100 μM $BzATP_o$ at 400 s increased Ca^{2+} influx. The upper graph shows a single-cell trace, while the lower graph presents average $[Ca^{2+}]_i$ profiles (experiment 71595-13; Cell 19).

ATP^{4-} would open more purinoceptors, which would explain the increase in Ca^{2+} influx in cells that had already responded, as well as the recruitment of thymocytes not responding in higher $[Mg^{2+}{}_o]$. Nevertheless, other interpretations are possible. First, ATP-gated channels in thymocytes may open in a graded fashion as the concentration of agonist increases, allowing more Ca^{2+} to enter the cell. Second, since ectoATPases require $MgATP^{2-}$ as substrate, reducing $Mg^{2+}{}_o$ may inhibit nucleotide catabolism at the surface of thymocytes, allowing a buildup of ATP^{4-}. Finally, Mg^{2+} ions may directly block nucleotide-gated pathways, as suggested by Nuttle and Dubyak (1994). Therefore, a relief of block, measured as a rise in $[Ca^{2+}]_i$, would be observed as $[Mg^{2+}]_o$ is decreased.

Significance of ATP_o-mediated Ca^{2+} Influx in Thymocytes

Members of the P2X family of purinoceptors have been suspected of being associated with programmed death in cells of the immune system since the work of Brake et al. (1994), who demonstrated a 40% sequence similarity between RP-2 (Owens et al., 1991), a gene activated in rat thymocytes undergoing apoptosis, and a $P2X_1$ clone isolated from a PC12 cDNA expression library. A subsequent study by Chvatchko et al. (1996) bolstered this hypothesis by showing that $P2X_1$ mRNA and protein expression were upregulated in mouse thymocytes induced to die by superantigen staphylococcal enterotoxin B. In addition, dexamethasone-induced upregulation of $P2X_1$ mRNA was found to occur in rat (Chvatchko et al., 1996) but not mouse thymocytes (Koshiba et al., 1997). The purinoceptors we have characterized, identified as the $P2X_7$/P2Z subtype (Fig. 3), do not appear to link ATP_o with apoptosis in thymocytes, because terminally differentiated double positive cells are least sensitive to nucleotides. Similarly, Nagy et al. (1995) have shown that mature (medullary) thymocytes exhibit a greater permeability to propidium iodide (668 D) after ATP_o treatment than mixed populations, indicating pore function, which in turn suggests the involvement of $P2X_7$/P2Z purinoceptors. Since we studied the ATP_o response over a limited time course, we cannot exclude the possibility that ATP_o induces the expression of $P2X_1$ and/or $P2Y_2$ purinoceptors in terminally differentiated thymocytes, which may lead to programmed cell death.

The possible role of ATP_o in programmed cell death in the thymus has been hotly debated. So far, three different P2 purinoceptors have been detected in thymocytes at either the mRNA or protein level, or by responses to ATP_o stimulation ($P2Y_2$, $P2X_1$, $P2X_7$/P2Z, respectively). The behavior of these multiple receptor subtypes may be responsible for the varied results in the literature. For instance, estimates of the molecular weight cutoff for the pore function attributable to $P2X_7$/P2Z purinoceptors in thymocytes vary between laboratories, ranging from a low value of 200 D (methylglucamine; Pizzo et al., 1991) through 314 D (ethidium; El-Moatassim et al., 1989*a*; Chused et al., 1996), and finally to a high limit of 668 D (propidium; Nagy et al., 1995). Two of these reports (Nagy et al., 1995; Chused et al., 1996) demonstrate that mature thymocytes are more permeable to the tested compound than immature precursors. Furthermore, steroid-induced expression patterns of mRNA for $P2Y_2$ and $P2X_1$ subtypes appear to be species dependent; two laboratories have shown $P2X_1$ mRNA expression in rat thymocytes (Chvatchko et al., 1996; Koshiba et al., 1997), suggesting that $P2X_1$ has RP-2–like activity. In contrast, dexamethasone induces $P2Y_2$, but not $P2X_1$ mRNA expression in mouse thymocytes (Koshiba et al., 1997). In not one report has a causal relationship between ATP_o and apoptosis been conclusively demonstrated. In addition, it has been sugggested that ATP_o may antagonize the apoptotic process in thymocytes, by a yet unknown process (Apasov et al., 1995). An alternative role for acute ATP_o stimulation and the consequent Ca^{2+} rise in thymocytes may be to drive cellular differentiation rather than trigger cell death.

Based upon our results we suggest that ATP_o acts as a generalized signal for growth and differentiation in lineages of thymocytes destined to become mature T cells. In our scheme, double negative cells in the outer cortex of the thymus are driven to differentiate by ATP_o, which would be expected to be at relatively low levels. It has been shown that before TCR expression, double-negative thymocytes are resistant to dexamethasone-induced (Cohen et al., 1993) or Ca^{2+}-mediated (Andjelic et al., 1993) apoptosis. As cells progress into the inner layers of the cortex and differentiate into double-positive thymocytes, they associate in tightly packed cell clusters (Kyewski et al., 1987). As many of these cells undergo apoptosis, high levels of ATP_o would be released. At this point in thymocyte development, it would be critical for double positive thymocytes, if they are to survive, to lose any response that would lead to high $[Ca^{2+}]_i$. Terminally differentiated double-positive thymocytes that are triggered by other means to begin programmed cell death regain an ATP_o response through the expression of $P2X_1$ and/or $P2Y_2$ pu-

rinoceptors, perhaps to accelerate the process by elevating intracellular Ca^{2+}. Cells that survive selection in the inner cortex and reach the medulla as single positive precursors to mature T lymphocytes would again be able to respond to ATP_o without danger of undergoing inadvertent cell death. As ATP_o levels are expected to be low in the medulla, these cells would upregulate the expression of $P2X_7$/P2Z purinoceptors.

Ca^{2+}-mediated signaling pathways have been implicated in the positive selection of double positive thymocytes driven by the interaction of αβ-TCR and MHC (for review see Jameson et al., 1995; Guidos, 1996). For example, inhibition of calcineurin, a calcium- and calmodulin-dependent phosphatase, by FK506, specifically blocks positive but not negative selection of $CD4^+CD8^+$ thymocytes in mice (Wang et al., 1995). Elevation of $[Ca^{2+}]_i$ by ionomycin in conjunction with protein kinase C activation can bypass the requirement for TCR engagement in positive selection leading to mature $CD4^+CD8^-$ thymocytes from mutant TCR-αβ–deficient $CD4^+CD8^+$ cells (Takehama and Nakauchi, 1996). Eichmann (1995) suggested that the magnitude of Ca^{2+} signal required for differentiation is increased during the progression toward more mature phenotypes. In addition, sensitivity to calcium-mediated apoptosis begins as thymocytes express molecules responsible for thymic selection (Andjelic et al., 1993). Our data demonstrate differential $[Ca^{2+}]_i$ responses to ATP_o among thymocyte subsets; both the probability and intensity of ATP-induced Ca^{2+} signals are reduced in small, double-positive thymocytes, relative to all other subsets. Thus, we suggest that ATP_o is not a specific trigger for programmed cell death in the thymus, but rather that ATP_o-stimulated $[Ca^{2+}]_i$ responses may act alone or in combination with TCR/MHC-stimulated signals to drive differentiation and positive selection of thymocytes.

We thank Dr. Miriam Ashley-Ross for extended discussions during manuscript preparation.

This work was supported by National Institutes of Health grants NS14609 and GM41514.

Received for publication 4 April 1997 and in revised form 1 July 1997.

References

Andjelic, S., N. Jain, and J. Nikolic-Zugic. 1993. Immature thymocytes become sensitive to calcium-mediated apoptosis with the onset of CD8, CD4, and the T cell receptor expression: a role for *bcl-2*? *J. Exp. Med.* 178:1745–1751.

Apasov, S., M. Koshiba, F. Redegeld, and M.V. Sitkovsky. 1995. Role of extracellular ATP and P1 and P2 classes of purinergic receptors in T-cell development and cytoxic T lymphocyte effector functions. *Immunol. Rev.* 146:5–19.

Barankiewicz, J., H.-M. Dosch, and A. Cohen. 1988. Extracellular nucleotide catabolism in human B and T lymphocytes. The source of adenosine production. *J. Biol. Chem.* 263:7094–7098.

Brake, A.J., M.J. Wagenbach, and D. Julius. 1994. New structural motif for ligand-gated ion channels defined by an ionotropic ATP receptor. *Nature (Lond.).* 371:519–523.

Bretschneider, F., M. Klapperstuck, M. Lohn, and F. Markwardt. 1995. Nonselective cationic currents elicited by extracellular ATP in human B-lymphocytes. *Pflugers Arch.* 429:691–698.

Buisman, H.P., T.H. Steinberg, J. Fischbarg, S.C. Silverstein, S.A. Vogelzang, C. Ince, D.L. Ypey, and P.C.J. Leijh. 1988. Extracellular ATP induces a large nonselective conductance in macrophage plasma membrane. *Proc. Natl. Acad. Sci. USA.* 85:7988–7992.

Burnstock, G. 1978. A basis for distinguishing two types of purinergic receptors. *In* Cell Membrane Receptors for Drugs and Hormones: A Multidisciplinary Approach. R.W. Straub and L. Bolis, editors. Raven Press, New York. 107–118.

Chused, T.M., S. Apasov, and M. Sitkovsky. 1996. Murine T lymphocytes modulate activity of an ATP-activated P_{2Z}-type purinoceptor during differentiation. *J. Immunol.* 157:1371–1380.

Chvatchko, Y., S. Valera, J.-P. Aubry, T. Renno, G. Buell, and J.-Y. Bonnefoy. 1996. The involvement of an ATP-gated ion channel, P_{2X1}, in thymocyte apoptosis. *Immunity.* 5:275–283.

Cockcroft, S., and B.D. Gomperts. 1979*a.* ATP induces nucleotide permeability in rat mast cells. *Nature (Lond.).* 279:541–542.

Cockcroft, S., and B.D. Gomperts. 1979*b.* Activation and inhibition of calcium-dependent histamine secretion by ATP ions applied to rat mast cells. *J. Physiol. (Lond.).* 296:229–243.

Cohen, G.M., X.-M. Sun, R.T. Snowden, M.G. Ormerod, and D. Dinsdale. 1993. Identification of a transitional preapoptotic population of thymocytes. *J. Immunol.* 151:566–574.

Collo, G., R.A. North, E. Kawashima, E. Merlo-Pich, S. Neidhart, A. Surprenant, and G. Buell. 1996. Cloning of $P2X_5$ and $P2X_6$ receptors and the distribution and properties of an extended family of ATP-gated ion channels. *J. Neurosci.* 16:2495–2507.

Coutinho-Silva, R., L.A. Alves, A.C.C. de Carvalho, W. Savino, and P.M. Persechini. 1996. Characterization of P_{2Z} purinergic receptors on phagocytic cells of the thymic reticulum in culture. *Biochim. Biophys. Acta.* 1280:217–222.

Dornand, J., M. Monis, and A. Dupuy D'Angeac. 1986. 5′-Nucleotidase activity of murine T-cell subpopulations separated according to their Lyt2 and L3T4 phenotypes. *Cell. Immunol.* 103:133–139.

Dubyak, G.R., and C. El-Moatassim. 1993. Signal transduction via P_2-purinergic receptors for extracellular ATP and other nucleotides. *Am. J. Physiol.* 265:C577–C606.

Eichmann, K. 1995. A signal strength hypothesis of thymic selection: preliminary considerations. *Immunol. Lett.* 44:87–90.

El-Moatassim, C., and G.R. Dubyak. 1992. A novel pathway for the activation of phospholipase D by P2Z purinergic receptors in BAC1.2F5 macrophages. *J. Biol. Chem.* 267:23664–23673.

El-Moatassim, C., J. Dornand, and J.-C. Mani. 1987. Extracellular ATP increases cytosolic free calcium in thymocytes and initiates the blastogenesis of the phorbol 12-myristate 13-acetate-treated medullary population. *Biochim. Biophys. Acta.* 927:437–444.

El-Moatassim, C., N. Bernad, J.-C. Mani, and J. Dornand. 1989*a.* Extracellular ATP induces a nonspecific permeability of thymocyte plasma membranes. *Biochem. Cell Biol.* 67:495–502.

El-Moatassim, C., T. Maurice, J.-C Mani, and J. Dornand. 1989*b.* The $[Ca^{2+}]_i$ increase induced in murine thymocytes by extracellular ATP does not involve ATP hydrolysis and is not related to phosphoinositide metabolism. *FEBS Lett.* 242:391–396.

Gonzalez, F.A., A.H. Ahmed, K.D. Lustig, L. Erb, and G.A. Weissman. 1989. Permeabilization of transformed mouse fibroblasts by 3′-*O*-(4-benzoyl)benzoyl adenosine 5′-triphosphate and the desensitization of the process. *J. Cell. Physiol.* 139:109–115.

Gordon, J.L. 1986. Extracellular ATP: effects, sources and fate. *Biochem. J.* 233:309–319.

Gregory, S.H., and M. Kern. 1978. Adenosine and adenine nucleotides are mitogenic for mouse thymocytes. *Biochem. Biophys. Res. Commun.* 83:1111–1116.

Gregory, S.H., and M. Kern. 1981. Mitogenic response of T-cell subclasses to agarose-linked and to free ribonucleotides. *Immunology.* 42:451–457.

Grynkiewicz, G., M. Poenie, and R.Y. Tsien. 1985. A new generation of Ca^{2+} indicators with greatly improved fluorescence properties. *J. Biol. Chem.* 260: 3440–3450.

Guidos, C.J. 1996. Positive selection of $CD4^+$ and $CD8^+$ T cells. *Curr. Opin. Immunol.* 8:225–232.

Harden, T.K., J.L. Boyer, and R.A. Nicholas. 1995. P_2-Purinergic receptors: subtype-associated signaling responses and structure. *Annu. Rev. Pharmacol. Toxicol.* 35:541–579.

Heppel, L.A., G.A. Weisman, and I. Friedberg. 1985. Permeabilization of transformed cells in culture by external ATP. *J. Membr. Biol.* 86:189–196.

Ikehara, S., R.N. Pahwa, D.G. Lunzer, R.A. Good, and M.J. Modak. 1981. Adenosine 5′-triphosphate- (ATP) mediated stimulation and suppression of DNA synthesis in lymphoid cells. I. Characterization of ATP responsive cells in mouse lymphoid organs. *J. Immunol.* 127:1834–1838.

Jameson, S.C., K.A. Hogquist, and M.J. Bevan. 1995. Positive selection of thymocytes. *Annu. Rev. Immunol.* 13:93–126.

Jiang, S., S.C. Chow, P. Nicotera, and S. Orrenius. 1994. Intracellular Ca^{2+} signals activate apoptosis in thymocytes: studies using the Ca^{2+}-ATPase inhibitor thapsigargin. *Exp. Cell Res.* 212:84–92.

Koshiba, M., S. Apasov, V. Sverdlov, P. Chen, L. Erb, J.T. Turner, G.A. Weisman, and M.V. Sitkovsky. 1997. Transient up-regulation of $P2Y_2$ nucleotide receptor mRNA expression is an immediate early gene response in activated thymocytes. *Proc. Natl. Acad. Sci. USA.* 94:831–836.

Kyewski, B.A., F. Momberg, and V. Schirrmacher. 1987. Phenotype of stromal cell-associated thymocytes in situ is compatible with selection of the T cell repertoire at an "immature" stage of thymic T cell differentiation. *Eur. J. Immunol.* 17:961–967.

Mahaut-Smith, M.P., and M.J. Mason. 1991. Ca^{2+}-activated K^+ channels in rat thymic lymphocytes: activation by concanavalin A. *J. Physiol.* 439:513–528.

Matko, J., P. Nagy, G. Panyi, G. Vereb, Jr., L. Bene, L. Matyus, and S. Damjanovich. 1993. Biphasic effect of extracellular ATP on the membrane potential of mouse thymocytes. *Biochem. Biophys. Res. Commun.* 191:378–384.

Nagy, P., G. Panyi, A. Jenei, L. Bene, R. Gaspar, Jr., J. Matko, and S. Damjan-

ovich. 1995. Ion-channel activities regulate transmembrane signaling in thymocyte apoptosis and T-cell activation. *Immunol. Lett.* 44:91–95.

Naumov, A.P., E.V. Kaznacheyeva, K.I. Kiselyov, Y.A. Kuryshev, A.G. Mamin, and G.N. Mozhayeva. 1995. ATP-activated inward current and calcium-permeable channels in rat macrophage plasma membranes. *J. Physiol.* 486:323–337.

North, R.A. 1996. P2X purinoceptor plethora. *Semin. Neurosci.* 8:187–194.

Nuttle, L.C., and G.R. Dubyak. 1994. Differential activation of cation channels and non-selective pores by macrophage P_{2Z} purinergic receptors expressed in *Xenopus* oocytes. *J. Biol. Chem.* 269:13988–13996.

Nuttle, L.C., C. El-Moatassim, and G.R. Dubyak. 1993. Expression of the pore-forming P_{2Z} purinoreceptor in *Xenopus* oocytes injected with Poly(A)$^+$ RNA from murine macrophages. *Mol. Pharmacol.* 44:93–101.

Osipchuk, Y., and M. Cahalan. 1992. Cell-to-cell spread of calcium signals mediated by ATP receptors in mast cells. *Nature (Lond.).* 359:241–244.

Osborne, B.A. 1996. Apoptosis and the maintenance of homeostatis in the immune system. *Curr. Opin. Immunol.* 8:245–254.

Owens, G.P., W.E. Hahn, and J.J. Cohen. 1991. Identification of mRNAs associated with programmed cell death in immature thymocytes. *Mol. Cell Biol.* 11:4177–4188.

Pizzo, P., P. Zanovello, V. Bronte, and F. Di Virgilio. 1991. Extracellular ATP causes lysis of mouse thymocytes and activates a plasma membrane ion channel. *Biochem. J.* 274:139–144.

Ross, P.E., and M.D. Cahalan. 1995. Ca^{2+} influx pathways mediated by swelling or stores depletion in mouse thymocytes. *J. Gen. Physiol.* 106:415–444.

Scollay, R., A. Wilson, A. D'Amico, K. Kelly, M. Egerton, M. Pearse, L. Wu, and K. Shortman. 1988. Developmental status and reconstitution potential of subpopulations of murine thymocytes. *Immunol. Rev.* 104:81–120.

Soltoff, S.P., M.K. McMillian, and B.R. Talamo. 1992. ATP activates a cation-permeable pathway in rat parotid acinar cells. *Am. J. Physiol.* 262:C934–C940.

Surprenant, A., F. Rassendren, E. Kawashima, R.A. North, and G. Buell. 1996. The cytolytic P_{2Z} receptor for extracellular ATP identified as a P_{2X} receptor ($P2X_7$). *Science (Wash. DC).* 272:735–738.

Steinberg, T.H., and F. Di Virgilio. 1991. Cell-mediated cytotoxicity: ATP as an effector and the role of target cells. *Curr. Opin. Immunol.* 3:711–715.

Takahama, Y., and H. Nakauchi. 1996. Phorbol ester and calcium ionophore can replace TCR signals that induce positive selection of CD4 T cells. *J. Immunol.* 157:1508–1513.

Tatham, P.E.R., and M. Lindau. 1990. ATP-induced pore formation in the plasma membrane of rat peritoneal mast cells. *J. Gen. Physiol.* 95:459–476.

Valera, S., N. Hussy, R.J. Evans, N. Adami, R.A. North, A. Surprenant, and G. Buell. 1994. A new class of ligand-gated ion channel defined by P_{2X} receptor for extracellular ATP. *Nature (Lond.).* 371:516–519.

Wang, C.R., K. Hashimoto, S. Kubo, T. Yokochi, M. Kubo, M. Suzuki, K. Suzuki, T. Tada, and T. Nakayama. 1995. T cell receptor-mediated signaling events in $CD4^+CD8^+$ thymocytes undergoing thymic positive selection but not negative selection. *J. Exp. Med.* 181:927–941.

Wiley, J.S., and G.R. Dubyak. 1989. Extracellular adenosine triphosphate increases cation permeability of chronic lymphocytic leukemic lymphocytes. *Blood.* 73:1316–1323.

Wiley, J.S., R. Chen, and G.P. Jamieson. 1993. The ATP^{4-} receptor-operated channel (P_2Z class) of human lymphocytes allows Ba^{2+} and ethidium$^+$ uptake: inhibition of fluxes by suramin. *Arch. Biochem. Biophys.* 305:54–60.

Wiley, J.S., J.R. Chen, M.B. Snook, and G.P. Jamieson. 1994. The P_{2Z}-purinoceptor of human lymphocytes: actions of nucleotide agonists and irreversible inhibition by oxidized ATP. *Br. J. Pharmacol.* 112:946–950.

Zhivotovsky, B., B. Cedervall, S. Jiang, P. Nicotera, and S. Orrenius. 1994. Involvement of Ca^{2+} in the formation of high molecular weight DNA fragments in thymocyte apoptosis. *Biochem. Biophys. Res. Commun.* 202:120–127.